

# Image Super-resolution via Hybrid NEDI and Wavelet-based Scheme

Zhi-Song Liu, Wan-Chi Siu and Jun-Jie Huang

Center for Signal Processing, Department of Electronic and Information Engineering  
Hong Kong Polytechnic University, Hong Kong

**Abstract**—This paper proposes to make super-resolution for low-resolution image via a hybrid scheme making use of the wavelet domain processing and the New Edge-Directed Interpolation (NEDI). The proposed method combines the accurate low frequency information obtained from the wavelet transform and phase-free high frequency information predicted from the Shift-Free NEDI (SF-NEDI). The underlying idea of this approach is to study the pixel shift caused by the wavelet transform and to fix this problem when using the SF-NEDI to enlarge image, such that more accurate high frequency information can be extracted from the enlarged image. By using the framework of wavelet transform, the proposed approach uses the original low-resolution image and high frequency information from the SF-NEDI to realize image super-resolution. Extensive experimental results show that the proposed hybrid approach can achieve about 0.7 dB improvement in peak signal-to-noise ratio over the Wavelet Zero-padding and 1.35 dB over the SF-NEDI.

**Keywords** - Image processing, Image super-resolution, New Edge-Directed Interpolation (NEDI), pixel shift, wavelet transform

## I. INTRODUCTION

Image super-resolution is a wide subject in image processing. Its goal is to obtain high-resolution (HR) images from blurred and noisy down-sampled low-resolution (LR) or natural images. Its applications in HDTV and video scalable coding [1] [2] have drawn a lot of attention. However, since with limited information about LR images, getting HR image is an ill-posed problem. Hence, to study the model of retrieving LR image can help to do super-resolution more accurately.

Image super-resolution can be categorized into two groups: spatial domain method [3]-[16], and transform domain methods [12]-[27].

Spatial domain method is one type of super-resolution where the LR image is down-sampled from the HR image in the spatial domain usually with/without an anti-aliasing pre-filtering. One special type of spatial domain methods is interpolation, for which the LR image is directly down-sampled from the HR image without any anti-aliasing pre-filtering. The advantage of interpolation is that it can predict the missing pixels from ground-truth LR pixels and the enlarged image can make sure one quarter (if  $2 \times 2$  enlargement) of pixels are from the original image. Methods of interpolation can be categorized into three groups: polynomial based methods [3]-[6], edge directed methods [7]-[8] and learning-based methods [9]-[11]. From these methods,

polynomial based methods are the simplest and fastest methods. On the contrary, learning-based methods have complicated learning process to slow down the speed in order to obtain outstanding results. Edge directed methods make use of the statistical estimation within local structure to predict edges and textures. The new edge-directed interpolation (NEDI) based methods [7] have proven to be useful in many cases. Besides interpolation, most of the general spatial domain methods consider to obtain the LR image from the degraded HR image, for which the HR image is blurred, noisy and/or down-sampled by specific kernels. Reference [12] summarizes the model to describe the whole degradation process of HR image. Based on this model, many statistic-based methods [12]-[17] make use of LR characters to predict HR images. Usually, they include up-sampling, deblurring and denoising steps to obtain the super-resolution (SR) image. For deblurring and denoising steps, to reach a better visual quality, many methods use iterative scheme or more than one single LR image to collect more useful information to do super-resolution. For example, reference [12] uses different blurring kernels and point spread functions to obtain several LR images and make use of them to reconstruct one HR image. Reference [17] uses a two-phase iterative scheme to optimize the MAP-POCS (Maximum a Posteriori Probability - Projection onto Convex Sets) method. Hence, to better reconstruct the HR image from this type of down-sampling method, more processing stages and/or better LR information are required.

Transform domain methods use known transform approaches to down-sample HR image without adding random noise, point spread functions or blurring filters for which pixels of the resultant LR image are transformed version of the original HR pixels. Usually, LR pixels are related to the nearest few HR pixels. Two major approaches are DCT-based super-resolution [18]-[23] and wavelet-based super-resolution [24]-[29]. References [21]-[23] make explicit explanation on how to combine DCT zero-padding with the 6-tap Wiener filter to obtain a better result. Using the same model of DCT-based super-resolution, [24]-[29] give further study on wavelet-based methods. [27] illustrates how to use cycle spinning to modify the ringing artifacts that happens after the DWT Zero-padding. It improves the visual quality but the improvement of PSNR is limited. Similar to [21], [29] proposes how to combine discrete wavelet transform with stationary wavelet transform or DCT transform to enhance the resolution of the LR image, which gives a promising direction for using wavelet transform to do super-resolution. The contribution of [29] is that it uses the stationary wavelet transform (SWT) to correct phase shift caused by discrete

wavelet transform (DWT) since stationary wavelet transform is undecimated version of DWT such that the hybrid scheme manages to improve the PSNR. However, using SWT does not obtain any new high frequency information and it only fixes phase shift of low frequency instead of high frequency.

The motivation of this paper is to make use of the wavelet transform to do super-resolution via the NEDI. We assume that the LR image is a down-sampled version of the HR image via the wavelet transform. It is interesting to note that most of wavelet-based methods are based on the assumption that the LR image is obtained from direct down-sampling, or generally blurred and noised down-sampling. There are very few papers talking about the super-resolution based on the LR down-sampled from the DWT for reference. In this paper, to discuss the super-resolution situation in wavelet domain, the HR image is down-sampled via Daubechies 4 wavelet transform [26]. After getting the LR image, step one is to interpolate the LR image by the NEDI. Step two is to use the Bicubic to calculate pixels at ground-truth positions by using pixels obtained from step one and the LR pixels to resolve the pixel shift problem. Step three is to perform wavelet transform on the image obtained from step two to get LL, LH, HL and HH parts. Making use of LH, HL and HH with the LR image, we can perform inverse wavelet transform to obtain the HR image.

The major contribution of this work can be summarized into two points. (1) We propose the Shift-Free NEDI (SF-NEDI) which resolves the pixel shift problem caused by wavelet down-sampling. The PSNR of image up-sampling by the SF-NEDI is 0.31 dB better than the SF-Bicubic (SF-Bicubic) and 0.541 better than the NEDI. (2) Since the LR image is the wavelet transformed version of the original image. The resultant enlarged image obtained from SF\_NEDI fixes the pixel shift but it calculates the high frequency information based on wavelet transformed version pixels. To further improve the spatial quality of the HR image, we improve the super-resolution performance by using the DWT to extract the high frequency information from the shift-free NEDI up-sampled image and combine it with the true wavelet down-sampled LR image as low frequency component to perform the inverse DWT to reconstruct HR image. The PSNR of the final image is on average 1.35 dB better than image up-sampled by SF-NEDI.

The rest of the paper is organized as follows: Section 2 gives the formulation of wavelet domain super-resolution and the proposed improvements. Section 3 presents the experimental results and section 4 concludes the paper.

## II. HYBRID NEDI-WAVELET BASED SCHEME

### A. DWT-based down-sampling

There are many wavelets and scaling functions [26] available to be selected to perform wavelet transform. The simplest one is the Haar wavelet which only needs two coefficients for low-pass filter and high-pass filter. From tests, we find that the Haar wavelet down-sampling is similar to down-sampling by averaging. Its ability of saving low frequency information is not as good as Daubechies 4 wavelet. Besides, using Daubechies 4 wavelet, its 4-coefficients of the low/high filters overlap every two HR pixels, such that LR

pixels contain correlation information. In the spatial domain, let us denote  $\mathbf{X}(n \times n)$  as the low-resolution (LR) image,  $\mathbf{Y}(2n \times 2n)$  as the high-resolution (HR) image,  $\mathbf{Y}^*((2n+2) \times (2n+2))$  as the boundary extension version of  $\mathbf{Y}$  and  $\mathbf{L}(n \times (2n+2))$  as the low-pass filter matrix. The down-sampling process can be explained in matrix equation as follows

$$X = \frac{1}{2} W Y W^T \tag{1}$$

$$x = \frac{1}{2} [h_1 \ h_2 \ h_3 \ h_4] \times \begin{bmatrix} y_{11} & y_{12} & y_{13} & y_{14} \\ y_{21} & y_{22} & y_{23} & y_{24} \\ y_{31} & y_{32} & y_{33} & y_{34} \\ y_{41} & y_{42} & y_{43} & y_{44} \end{bmatrix} \times \begin{bmatrix} h_1 \\ h_2 \\ h_3 \\ h_4 \end{bmatrix} \tag{2}$$

Equation (2) shows the relationship between one LR pixel  $x$  and HR pixel  $y$ ,  $x$  is correlated with nearest  $y$  by low-pass filter coefficients. Since the discrete wavelet transform samples every two data, each LR pixel can be considered at the center of nearest four HR pixels. This gives us the idea how pixel shift happens in DWT down-sampling.

### B. DWT Zero-Padding

Let us use figure 1 to illustrate the DWT Zero-padding (WZP) process. Assume that the LR image down-sampled by the wavelet transform is available in the spatial domain. Let us multiple the LR image by 2 and pad zeros at LH, HL and HH components. The combined block is then performed inverse DWT transformed to obtain the HR image in the spatial domain.

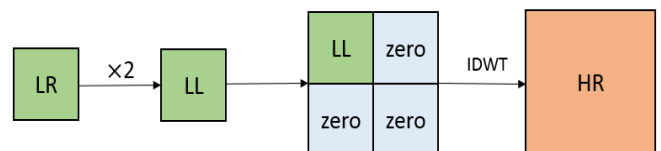


Figure 1. DWT zero-padding process

### C. Shift-free NEDI method to solving pixel shift

NEDI [7] makes use of the geometric duality property to estimate HR covariance by LR covariance and interpolates the HR pixels using estimated covariance.

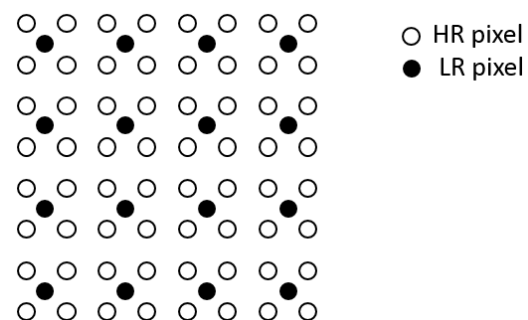


Figure 2. Spatial coordinates of the LR pixels

To use the down-sampled DWT image, let us check the pixel shift caused by DWT down-sampling in figure 2. Each

LR pixel is the sum of weighted nearest  $4 \times 4$  HR pixels. After using NEDI to perform interpolation, we get the enlarged image in figure 3, where  $\blacktriangle$  is the estimated NEDI pixel. Note that each estimated NEDI pixel has shifted from original HR pixel coordinates. This shift affects the whole image with serious errors. In order to eliminate this shift effect, we make use of the Bicubic [3] approach again to interpolate the pixel values in the original positions (the grey dots (pixels) in Fig.4). For example, pixel  $x$  is obtained by making use of its nearest  $4 \times 4$  available pixels, including 12 estimated NEDI pixels and 4 LR pixels in the square window of figure 4.

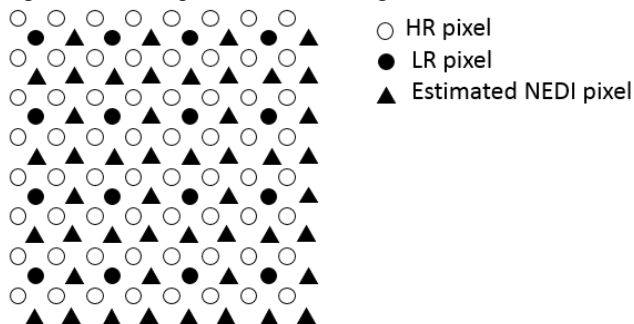


Figure 3. Spatial coordinates of the LR and NEDI pixels

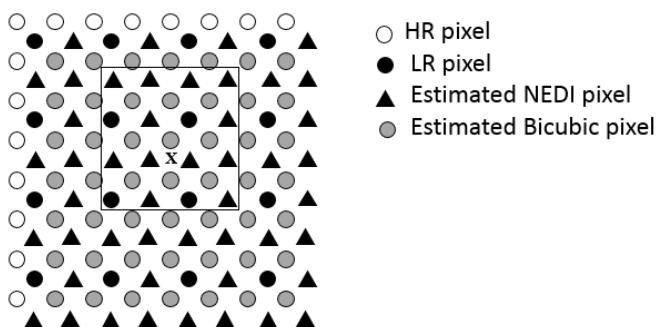


Figure 4. Spatial coordinates of the LR, NEDI and Bicubic pixels

To make a comparison, let us perform the Bicubic method to compare with the NEDI. Making arrangement the same as SF-NEDI, the LR image is also assumed to be obtained from performing DWT on the HR image.

To enlarge the LR image, there are two steps. (i) Step one is to perform the Bicubic interpolation, which is to obtain the step one Bicubic pixels ( $\nabla$ ) as shown in figure 5. (ii) Step two is the pixel shift correction stage, which performs Bicubic interpolation again, using LR pixels and step one Bicubic interpolated pixels in the square bracket as shown in figure 6. Note that both step one and step two have to perform the Bicubic method, but they evaluate pixels at different positions. To illustrate the improvement after solving the pixel shift problem, TABLE 1 shows the comparison between Bicubic, NEDI and their shift free methods. The improvement of PSNR is outstanding which leads us to take its advantage to improve reconstruction quality further.

*D. Hybrid NEDI-wavelet-based Scheme*

Using SF-NEDI instead of the NEDI to do super-resolution can improve the quality of HR image. However, NEDI works

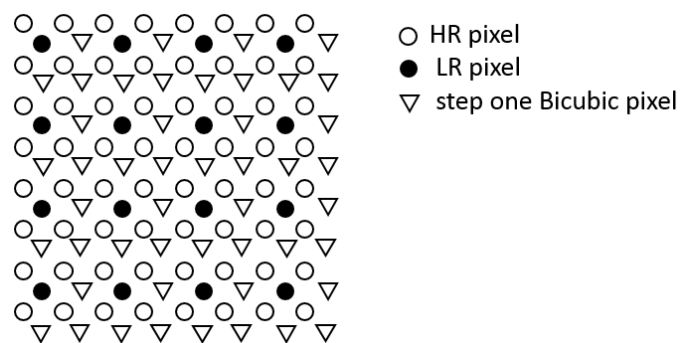


Figure 5. Spatial coordinates of the LR and step one Bicubic pixels

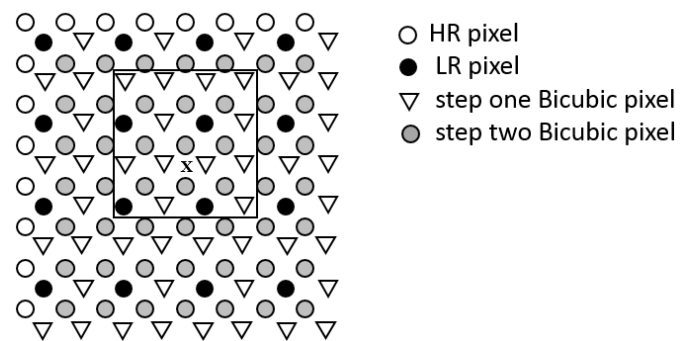


Figure 6. Spatial coordinates of the LR, step one Bicubic and step two Bicubic pixels

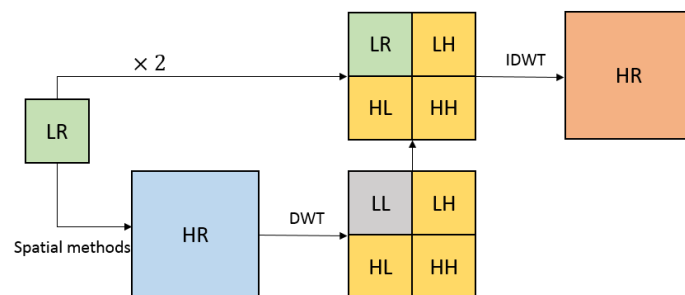


Figure 7. Hybrid Wiener-wavelet-based scheme

well in direct down-sampling for interpolation processing because it forms the right HR covariances by making use of the position matched LR covariances.

The fact for direct down-sampling methods is that it keeps one quarter of the original HR pixels as LR pixels, the rest of missing pixels are obtained based on known LR pixels. On the contrary, the initial step of SF-NEDI estimates missing pixels based on the result of wavelet down-sampled LR image so that the NEDI estimated pixels only reflect correlation between down-sampled LR pixels. It can represent the covariance of the wavelet version of the HR pixels instead of the HR pixels in the spatial domain. The same situation works for the shift-free Bicubic (SF-Bicubic). This can explain why the PSNR of DWT zero-padding is higher than that of the SF-NEDI and SF-Bicubic. To further improve reconstruction quality, let us modify the model brought out in [21] and [29] to combine the result of the SF-NEDI or the SF-Bicubic with DWT transform. The process is illustrated in figure 7. Step one uses the SF-NEDI or the SF-Bicubic to up-sample the LR

image to get the enlarged image. Step two performs DWT to the enlarged image to get LL, LH, HL and HH parts, and then combines the LR image multiplied by 2 with LH, HL and HH parts of the enlarged image in the wavelet domain. Step three performs the inverse DWT to combined image to get the HR image.

### III. EXPERIMENTAL RESULTS

To evaluate the proposed approach, 16 images (512×512) with various contents have been selected for testing. Figure 8 shows the gray level test images. Table 1 shows the PSNR (dB) comparison with different algorithms [3], [7] and [28] for 2×2 up-sampling. To eliminate the error around boundaries, the PSNR calculation range is from 4 to 509 instead of 1 to 512.

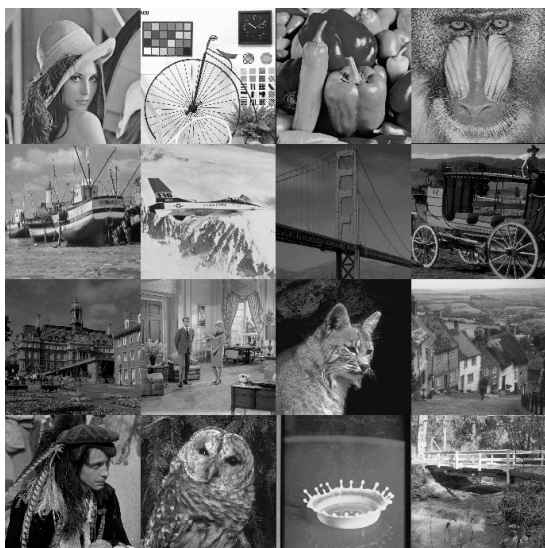


Figure 8. 16 testing images

In order to show the advantage after resolving the pixel shift, we use the Bicubic and NEDI to compare with our novel shift-free schemes for 2×2 super-resolution. From TABLE 1, the PSNR of SF-Bicubic is 0.35 dB better than the Bicubic. The PSNR of SF-NEDI is 0.54 dB better than the NEDI. It is interesting to note that SF-Bicubic is better than SF-NEDI which is similar to the case in direct down-sampling situation where using Bicubic to do interpolation is better than NEDI. For the Hybrid wavelet based scheme, there are few proper methods to compare with since our LR image obtained from the wavelet down-sampling and [24], [25], [28] and [29] use the wavelet based methods to enhance resolution without enlarging the size of the LR image. Only [27] can be used to compare with our methods. We use DWT Zero-padding, WZP-CS and the hybrid wavelet based scheme to do the same 2×2 super-resolution. For DWT Zero-padding, though we used the original low frequency information obtained from HR image, the high frequency components are filled with zeros. It does not help to recover the edges and textures. For WZP-CS, based on [27], when k=2 phase shifts can achieve a higher PSNR so that in TABLE 2, we can see the slight improvement of PSNR compared with DWT Zero-padding. For Hybrid scheme with DWT transform, it helps to transform the high

TABLE 1. PSNR OF 16 TESTING IMAGES WITH DIFFERENT ALGORITHMS WITH PIXEL SHIFT RESOLVED

Images	Bicubic[3]	Shift-Free Bicubic	NEDI[7]	Shift-free-NEDI
Lena	32.645	33.572	32.184	33.360
Baboon	23.783	23.716	23.502	23.608
Bicycle	21.019	21.035	21.244	21.282
Boat	29.339	29.613	29.827	29.354
Pepper	32.357	33.220	31.816	33.100
Goldhill	30.857	31.058	30.273	30.713
Couple	29.179	29.392	28.605	29.142
Stream	26.275	26.364	25.542	25.947
Splash	35.999	36.969	35.669	36.787
Man	28.485	28.715	27.948	28.385
Airplane	32.120	33.045	31.037	32.179
Bridge	34.465	34.469	33.909	34.201
Cart	28.174	28.471	27.539	28.211
Church	28.373	28.374	27.304	27.747
Flin	31.475	31.727	30.787	31.228
Owl	28.427	28.753	27.694	28.292
<b>Average PSNR</b>	29.561	29.906	29.055	29.596
<b>Improvement</b>	-	0.345	-	0.541

TABLE 2. THE PSNR OF 16 TESTING IMAGES WITH DIFFERENT ALGORITHMS WITH SOLVING PIXEL SHIFT

Images	DWT zero-padding	WZP-CS[27]	Shift Free Bicubic-wavelet-based method	Shift-free NEDI-wavelet-based method
Lena	33.859	34.231	34.888	<b>35.194</b>
Baboon	24.139	23.874	24.266	<b>24.429</b>
Bicycle	21.491	21.202	21.685	<b>22.211</b>
Boat	29.940	30.033	30.504	<b>30.675</b>
Pepper	33.513	33.693	34.201	<b>34.478</b>
Goldhill	31.477	31.400	31.770	<b>31.818</b>
Couple	29.774	29.723	30.302	<b>30.435</b>
Stream	26.747	26.640	<b>27.068</b>	27.038
Splash	37.243	37.585	38.119	<b>38.322</b>
Man	29.085	29.051	29.591	<b>29.689</b>
Airplane	33.140	33.678	<b>34.521</b>	34.362
Bridge	34.779	34.828	35.331	<b>35.465</b>
Cart	28.703	28.916	29.544	<b>29.770</b>
Church	28.812	28.807	<b>29.313</b>	29.160
Flin	31.980	32.040	<b>32.588</b>	32.574
Owl	29.021	29.112	<b>29.538</b>	29.533
<b>Average PSNR</b>	30.232	30.301	30.827	<b>30.947</b>
<b>Improvement</b>	-	0.069	0.595	0.715

frequency information obtained from SF-NEDI and SF-Bicubic in wavelet domain instead of spatial domain so that they can be used with the LR image to perform inverse wavelet transform. This improvement does not require too much computation cost or complicated algorithms so that this is an easy way to get better visual quality in practice. From Table 2, The PSNR of the WZP-CS improves very little but it helps to reduce the ringing artifacts. The PSNR of the Hybrid SF-Bicubic-wavelet-based scheme is 0.595 dB better than that of the DWT zero-padding, the Hybrid SF-NEDI scheme is 0.715 dB better than that of the WZP. These comparisons prove that using the shift-free schemes can help to evaluate useful high frequency information from the spatial interpolation methods to up-sample the LR images. Besides, using Hybrid SF-Bicubic-wavelet-based method is very similar to Hybrid SF-NEDI-wavelet-based method. Checking their differences between images, we find that for images with more edges or textures, the Hybrid SF-NEDI-wavelet-based method can improve the PSNR better than Hybrid SF-Bicubic-wavelet-based method. An explanation is that the NEDI evaluates the missing pixels by geometry duality. It can help to improve visual quality by reconstructing some curves and edges but the PSNR is no better than the Bicubic. For images with more edges and textures, using NEDI could evaluate more ground truth high frequency information so that when we perform wavelet transform to extract the high frequency parts LH, HL and HH, they would not degrade the image quality. On the contrary, for smoother images, like Bridge, using SF-Bicubic can improve the overall PSNR so that when we perform wavelet transform, the results are better than Hybrid SF-NEDI-wavelet-based method. In figure 9, it gives more visual details on comparing different methods for super-resolution. From this figure, DWT Zero-padding is blurring because of the loss of high frequency information. WZP-CS helps to reduce the ringing artifacts of WZP but also blurs the image. Compared to the SF-Bicubic, the SF-NEDI manages to reconstruct the edges and high frequency information. Using the proposed scheme, these blurring and noising effects are eliminated to some extents in visual observation. The results confirm the idea that using the SF-NEDI can improve the quality of image and using the Hybrid SF-NEDI-wavelet-based super-resolution is the best choice overall.

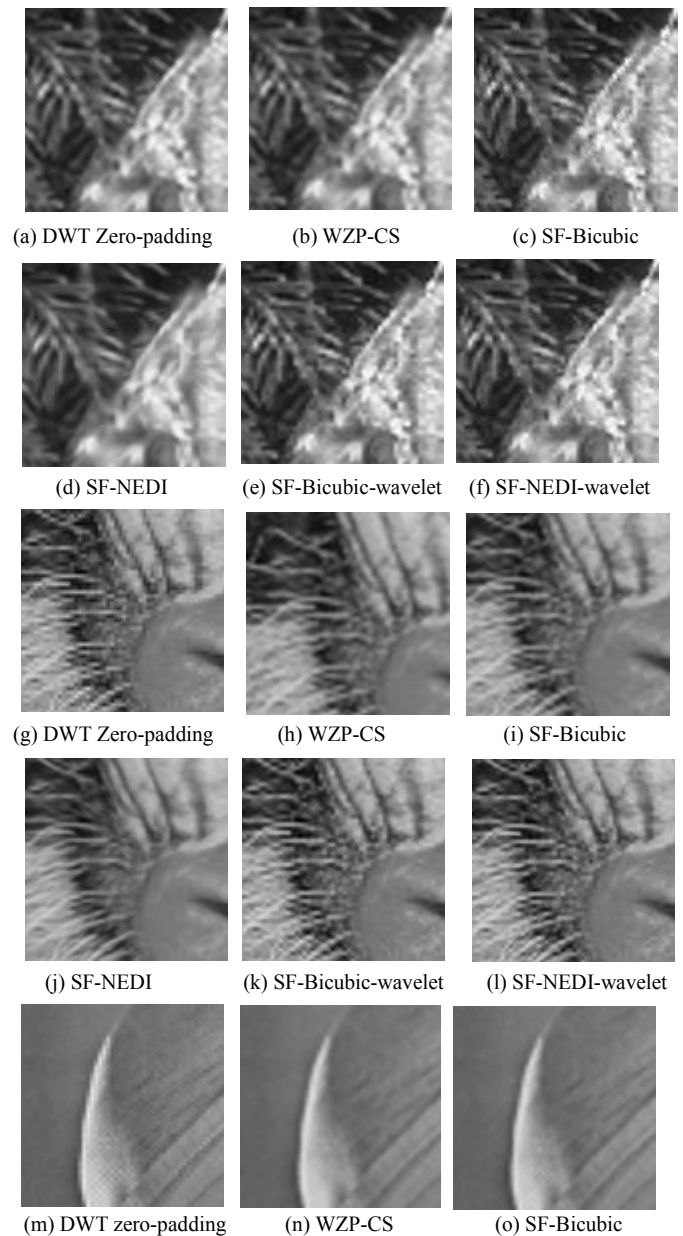
#### IV. CONCLUSION

A Hybrid-NEDI-wavelet-based scheme is proposed for image super-resolution. This paper discusses the pixel shift happening during the wavelet down-sampling. By resolving this problem, the NEDI can be effectively applied into image super-resolution. Besides, combining high frequency information from the shift-free-NEDI up-sampled image with the original LR image by performing the wavelet transform gives us more promising results. This hybrid approach is extremely useful for scalable image/video coding using the wavelet transform, for which the LR image is used as the base layer, whereas LH, HL and HH blocks obtained by making use of the discrete wavelet transform results of the spatially interpolated LR image (plus the required amount of residual signals) can form the enhancement layer. Details of the

scalable coding making use of this approach is part of our future work. Furthermore, we may also resolve the problem of pixel shift by other methods as a further investigation. Quality of the LR image can also be improved for super-resolution by using an iterative scheme. Another direction is to use other wavelet functions instead of Daubechies 4 to do down-sampling and up-sampling.

#### Acknowledgment

This work is supported by the Center for Signal Processing, the Hong Kong Polytechnic University (G-YBAS) and the Research Grant Council of the Hong Kong SAR Government: PolyU5243/13E(B-Q38S).



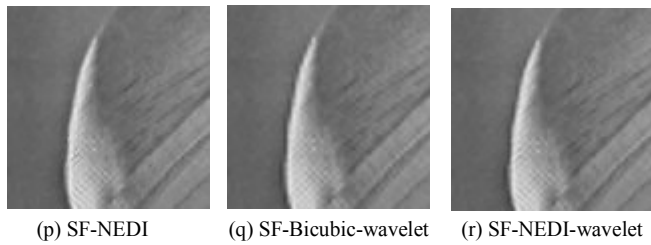


Figure 9. Subjective comparison of different methods

### References

[1] X. Wu, X. Zhang and X. Wang, "Low bit-rate image compression via adaptive down-sampling and constrained least squares upconversion", *IEEE Trans. Image Process.*, vol. 18, no. 3, pp. 552-561, Mar. 2009.

[2] Z. Shi, X. Sun and F. Wu, "Spatially Scalable Video Coding For HEVC," *IEEE Trans. Circuits Syst. Video Technol.*, vol.22, no.12, pp.1813-1826, Dec. 2012.

[3] R. Keys, "Cubic convolution interpolation for digital image processing," *IEEE Trans. Acoust., Speech, Signal Process.*, vol. 29, no. 6, pp. 1153-1160, Dec. 1981.

[4] H. S. Hou and H. Andrews, "Cubic splines for image interpolation and digital filtering," *IEEE Trans. Acoust., Speech, Signal Process.*, vol. 26, no. 6, pp. 508-517, Dec. 1978.

[5] T. Blu, P. Thevenaz, and M. Unser, "Linear interpolation revitalized," *IEEE Trans. Image Process.*, vol. 13, no. 6, pp. 710-719, May 2004.

[6] T. M. Lehmann, C. Gönnner, and K. Spitzer, "Addendum: B-spline interpolation in medical image processing," *IEEE Trans. Med. Imag.*, vol. 20, no. 7, pp. 660-665, Jul. 2001.

[7] X. Li and M. T. Orchard, "New edge-directed interpolation," *IEEE Trans. Image Process.*, vol. 10, no. 10, pp. 1521-1527, Oct. 2001.

[8] K.-W. Hung and W.-C. Siu, "Robust soft-decision interpolation using weighted least squares," *IEEE Trans. Image Process.*, vol. 21, no. 3, pp. 1061-1069, Mar. 2012.

[9] K. S. Ni and T. Q. Nguyen, "An adaptable k-nearest neighbors algorithm for MMSE image interpolation," *IEEE Trans. Image Process.*, vol. 18, no. 9, pp. 1976-1987, Sep. 2009.

[10] Y. Romano, M. Protter, and M. Elad, "Single image interpolation via adaptive nonlocal sparsity-based modeling," *IEEE Trans. Image Process.*, vol. 23, no. 7, pp. 3085-3098, May 2014.

[11] W. Dong, L. Zhang, R. Lukac, and G. Shi, "Sparse representation based image interpolation with nonlocal autoregressive modeling," *IEEE Trans. Image Process.*, vol. 22, no. 4, pp. 1382-1394, Apr. 2013.

[12] M. Elad, "Super-Resolution Reconstruction of Images," PhD thesis, Technion Israel Inst. of Technology, Dec. 1996.

[13] M. Elad and A. Feuer, "Restoration of Single Super-Resolution Image From Several Blurred, Noisy and Down-Sampled Measured Images", the *IEEE Trans. on Image Processing*, Vol. 6, no. 12, pp. 1646-58, December 1997.

[14] M. Elad and Y. Hel-Or, "A Fast Super-Resolution Reconstruction Algorithm for Pure Translational Motion and Common Space Invariant Blur", Accepted to the *IEEE Trans. on Image Processing*, March 2001.

[15] He He and Wan-Chi Siu. Single Image Super-resolution using Gaussian Process Regression. *IEEE Conference on Computer Vision and Pattern Recognition*. Jun 2011.

[16] Tao Wang, Yan Zhang and Li-Xia Lin. Automatic Superresolution Image Reconstruction Based on Hybrid MAP-POCS. *International Conference on Wavelet Analysis and Pattern Recognition*, vol. 1. Nov 2007.

[17] Liyakathunisa, L. and Kumar, C.N.R.A Novel Wavelet based Super Resolution Reconstruction of Low Resolution Images using Adaptive Interpolation. *International Conference on Advances in Recent Technologies in Communication and Computing*. Oct 2010. M. Young, *The Technical Writer's Handbook*. Mill Valley, CA: University Science, 1989.

[18] R. Dugad and N. Ahuja, "A fast scheme for image size change in the compressed domain," *IEEE Trans. Circuits Syst. Video Technol.*, vol. 11, no. 4, pp. 461-474, Apr. 2001.

[19] J. Mukherjee and S.K. Mitra, "Image resizing in the compressed domain using subband DCT," *IEEE Trans. Circuits Syst. Video Technol.*, vol.12, no.7, pp.620-627, Jul. 2002.

[20] H. W. Park, Y. S. Park, and S. K. Oh, "L/M-fold image resizing in block-DCT domain using symmetric convolution," *IEEE Trans. Image Process.*, vol. 12, no. 9, pp. 1016-1034, Sep. 2003.

[21] Zhenyu Wu, Hongyang Yu and Chang Wen Chen, "A New Hybrid DCT-Wiener-Based Interpolation Scheme for Video Intra Frame Up-Sampling," *IEEE Signal Processing Letters*, vol.17, no.10, pp.827-830, Oct. 2010.

[22] Kwok-Wai Hung and Wan-Chi Siu, "Hybrid DCT-Wiener-Based Interpolation via Learnt Wiener Filter", *Proceedings*, pp. 1419-1423, *IEEE International Conference on Acoustics, Speech, Signal Processing (ICASSP'2013)*, 26-31 May, 2013, Vancouver, Canada.

[23] Kwok-Wai Hung and Wan-Chi Siu, "Novel DCT-based Image Upsampling using Learning-based Adaptive k-NN MMSE Estimation", *IEEE Transactions on Circuit and Systems for Video Technology*, Vol. 24, No. 12, pp. 2018-2033, April, 2013.

[24] Y. Piao, I. Shin, and H. W. Park, "Image resolution enhancement using inter-subband correlation in wavelet domain," in *Proc. Int. Conf. Image Process.*, 2007, vol. 1, pp. 1-445-448.

[25] H. Demirel and G. Anbarjafari, "Satellite image resolution enhancement using complex wavelet transform," *IEEE Geoscience and Remote Sensing Letter*, vol. 7, no. 1, pp. 123-126, Jan. 2010.

[26] S. Mallat, *A Wavelet Tour of Signal Processing*, 2nd ed. New York: Academic, 1999.

[27] A. Temizerl and T. Vlachos, "Wavelet domain image resolution enhancement using cycle-spinning," *Electron. Lett.*, vol 41, no. 3, pp. 119-121, Feb. 3, 2005.

[28] S. G. Chang, Z. Cvetkovic and M. Vetterli "Locally adaptive wavelet-based image interpolation". *IEEE Trans. Image Process.*, vol. 15, no. 6, pp.1471 -1485 2006.

[29] H. Demirel and G. Anbarjafari "IMAGE resolution enhancement by using discrete and stationary wavelet decomposition". *IEEE Trans. Image Process.*, vol. 20, no. 5, pp.1458 -1460 2011.